COUNTER-CURRENT GAS/LIQUID FLOW THROUGH CHANNELS WITH CORRUGATED WALLS VISUAL OBSERVATIONS OF LIQUID DISTRIBUTION AND FLOODING

S.V. Paras , E.I.P. Drosos , A.J. Karabelas and F. Chopard*

Department of Chemical Engineering
and Chemical Process Engineering Research Institute
Aristotle University of Thessaloniki
Univ. Box 455, GR 540 06 Thessaloniki, GREECE

*Alfa Laval Vicarb
1-9 rue du Rif Tronchard, F38120 Le Fontanil Cornillon, FRANCE

Abstract: New data are reported and supported by visual observations and fast recordings on liquid distribution and flooding phenomena within flow channels simulating novel compact condensers. Experiments were carried out under adiabatic flow conditions with various liquids using a special test section simulating a vertical channel of a *corrugated* plate heat exchanger. The pressure drop was also measured between top and bottom of the channel. The observations suggest that the two side channels (machined on the plates) play a dominant role in liquid distribution, allowing the effective "drainage" of liquid moving in the lateral direction. Two critical flow conditions were identified, which are of considerable practical significance i.e. liquid "maldistribution" and flow reversal/flooding. The critical gas velocities of incipient "maldistribution" and of flooding tend to increase with decreasing liquid feed rate, as expected. Concerning fluid properties, significant differences are observed (compared to water) in the liquid film distribution and the flooding velocities with the lower interfacial tension butanol solution and kerosene. The latter is associated with the smallest critical flooding velocities measured. The pressure drop tends to increase with both the air and the liquid flow rates. Compared to water, a steeper increase of the pressure gradient is evident for the butanol mixture in the same range of flow conditions.

1. INTRODUCTION

In counter-current gas-liquid flow, the onset of flooding is identified as the maximum rate at which one phase can flow counter-currently with respect to the other. The phenomenon of flooding is of considerable technological importance being a limiting factor in the operation of various types of two-phase equipment including the very common reflux condensers. In the latter, flooding poses a major problem, hindering their smooth operation, as it is associated with choking of the upward moving vapors and with a sharp rise of pressure drop. Therefore, the design engineer needs reliable tools to determine the critical conditions leading to flooding as well as the region of smooth condenser operability. Such tools are unavailable at present mainly due to very limited work reported for narrow flow passages with corrugated walls. Novel compact condensers, and two-phase heat exchangers in general, made of *corrugated plates* hold significant advantages over conventional equipment. To better exploit these advantages and to optimize design and operation of this new equipment, there is a need to better understand liquid distribution and flooding phenomena within the flow channels. Therefore, it is the purpose of this work to study counter-current gas-liquid flow, under adiabatic conditions, in a vertical rectangular channel with corrugated walls in order to gain insight into the complicated flow field and to elucidate the flooding mechanisms, leading to reliable predictive methods.

A great deal of work has been carried out on flooding, in *vertical pipes* with smooth walls, and has been reviewed in a compehensive paper by Bankoff and Lee (1986). The latter as well as recent papers (e.g. Lacy and Dukler, 1994; Koizumi and Ueda, 1996; Ghiaasiaan et al., 1997; Wongwises and Thanaporn, 1998; etc.) show that the main factors influencing the onset of flooding are (in addition to conduit geometry) the type of fluid entrance and exit as well as the physical properties of both fluids.

The amount of work on counter-current flow in *vertical rectangular channels* is limited, particularly for a narrow gap between the vertical plates. Biage (1989) conducted flooding tests in a vertical channel with porous liquid inlet and outlet sections and a relative large channel gap (25 mm) between the main parallel plates. Osakabe and Kawasaki (1989) carried out "top flooding" experiments in thin rectangular passages (i.e. 10x100, 5x100 and 2x100 mm) motivated by problems in the nuclear industry. Their flow system, however, with a constant head pool of fluid above the channel top, is drastically different than the flow field in commercial plate heat exchangers (reflux condensers). Larson et al. (1994) reported experiments with similar liquid feeding conditions, in *very narrow* rectangular channels of 1.1 and 2.2 mm gap. Vlachos et al (2001) reported new flooding data obtained in a vertical rectangular channel with 5 and 10 mm gap between its main flat parallel plates. Such flow passages may be considered to simulate single flow "elements" of a compact reflux condenser made of flat plates.

Due to the complexity of the mechanisms involved, reliable predictive tools of general validity are not available at present, even for flooding in pipes (Bankoff and Lee, 1986). The most commonly used correlation for the flooding limit in vertical tubes, although quite often unsuccessfully, is due to Wallis (1969):

$$\sqrt{U_G^*}+C_1\sqrt{U_L^*}=C_2 \qquad (1)$$

where

$$U_G^* = U_G \sqrt{\frac{\rho_G}{gD(\rho_L - \rho_G)}}\,,\quad U_L^* = U_L \sqrt{\frac{\rho_L}{gD(\rho_L - \rho_G)}} \qquad (2)$$

with parameters C_1 = 0.8 - 1.0 and C_2 = 0.7 – 1.0, mainly depending on geometry. U_G and U_L are the gas and liquid superficial velocities respectively, ρ_G and ρ_L the phase densities, g the acceleration due to gravity and D the tube diameter. Vlachos et al (2001), on the basis of their data, report that a Wallis type correlation is inapplicable to the case of vertical channels of rectangular cross-section.

Zapke and Kroger (2000a) studied recently the effect of the duct geometry (the duct height and width varied from 50 to 150 mm and 10 to 20 mm, respectively) and fluid properties on flooding, using water, methanol, propanol and several gas phases. They concluded that the flooding gas velocity is strongly dependent on the duct height, the phase densities and duct inclination. The flooding gas velocity decreases with increasing liquid viscosity, which seems to have a stronger effect than the surface tension. Additionally, Zapke and Kroger (2000b) propose a number of flooding correlations involving dimensionless groups such as gas Froude number at flooding point, liquid Froude and Ohnesorge numbers. The validity of these correlations is uncertain at present.

To the best of the authors knowledge, there is no published work on *counter-current* gas/liquid flow through channels made of *corrugated plates*, which is of interest here in connection with compact reflux condenser operation. The recent study of Winkelmann et al (1999) deals with co-current air/water downflow through a corrugated-plate apparatus under adiabatic conditions. Yan et al (1999) report on condensation experiments (with the R-134a refrigerant) in vertical channels made of corrugated plates of the chevron type. By feeding the vapours at the top, co-current two-phase downflow prevailed in their test-section, different than the counter-current flow of interest to this study.

In the following, the experimental set-up and procedures are outlined first; the main results drawn from the flooding tests and visualization studies are presented and discussed next.

2. EXPERIMENTAL SET-UP AND PROCEDURE

An experimental facility was specifically built to study counter-current gas-liquid flow and to determine flooding conditions (**Figure 1**). Two-phase flow was developed in a special Plexiglas test section (formed by two plates 70 cm high and 15 cm wide), simulating a vertical channel of a corrugated plate heat exchanger. On the two plates manufactured by VICARB-Alfalaval, corrugations were machined at a 45^o angle, as well as side grooves, i.e. vertical side channels. The two plates were superposed so that the opposite corrugations formed a cross-type pattern with the crests of the corrugations nearly in contact. On each plate, a porous section was flush mounted at top and bottom, to feed and withdraw the liquid, respectively. The length of the test section, measured between the bottom edge of the inlet porous wall and the top edge of the outlet porous section, is 40 cm. The equipment includes a honeycomp and a smooth entrance section for the gas, and minimizes the possibility of artificially creating disturbance waves due to the liquid exit geometry. The liquid is collected in a 0.05 m^3 storage tank and is recirculated through the loop by means of a pump. On top of the measuring section there is a phase separator from which the liquid phase is fed back to the storage tank, whereas air is released to the atmosphere. This set-up allows good control of flow conditions and represents an idealized case of conditions prevailing in a single element of a compact heat exchanger.

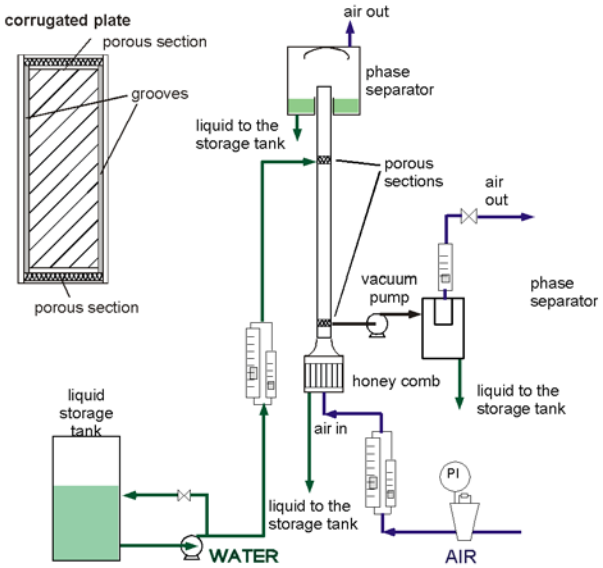

Figure 1. A schematic of the experimental set-up for studying countercurrent gas-liquid flow, with some details of a corrugated plate.

Experiments were carried out under adiabatic flow conditions with water, a water/butanol mixture (5%) and kerosene at ambient temperature (~ 20°C) (**Table 1**) and slightly elevated pressure (up to 1.1 bar absolute) maintained inside the test section, to facilitate liquid removal through the outlet porous wall section. A small amount of gas permeated the porous sections together with the liquid film removed and was measured by a rotameter after separating the two fluids using a phase separator and a vacuum pump. Each experiment was carried out by pre-pressurizing the channel with the gas flowing at a relatively low rate. Then, the required liquid flow rate was fixed and the liquid flowed steadily down to the outlet porous wall section where it exited the channel. Next, the gas flow rate was progressively increased until the onset of flooding.

Visual studies were made using a Redlake *Motion*Scope PCI® high-speed camera positioned outside the test section, either slightly above the liquid exit or below the liquid entrance section. For these experiments a recording rate of 500 fps was considered to be suitable. Pressure drop was measured across the test section using a differential pressure transducer connected to two pressure taps; data were acquired for 20 sec with a sampling frequency of 250 Hz.

Table 1. Properties of liquids used in the experiments.

	water	***5% butanol***	***kerosene***
μ, *kg m^{-1}s^{-1}*	0.001	0.00143	0.001333
ρ, *kg m^{-3}*	1000	986.7	775
σ, *kg s^{-2}*	0.07118	0.032	0.0268
contact angle, *deg*	32 (48)*	20 (*27*)*	0 (0)*
Oh$_L$	0.00147	0.00315	0.00363
Ka$_L$	3325	923	783

*on rough surface

3. RESULTS

Visual Observations- Flow Patterns

The flow patterns were observed by naked eye and were recorded by a high-speed camera. The physical properties of liquids employed in the tests are listed in Table 1. In **Figure 2** typical pictures of air-water counter-current flow are included, showing also the two critical conditions identified as *"maldistribution"* and *flooding*.

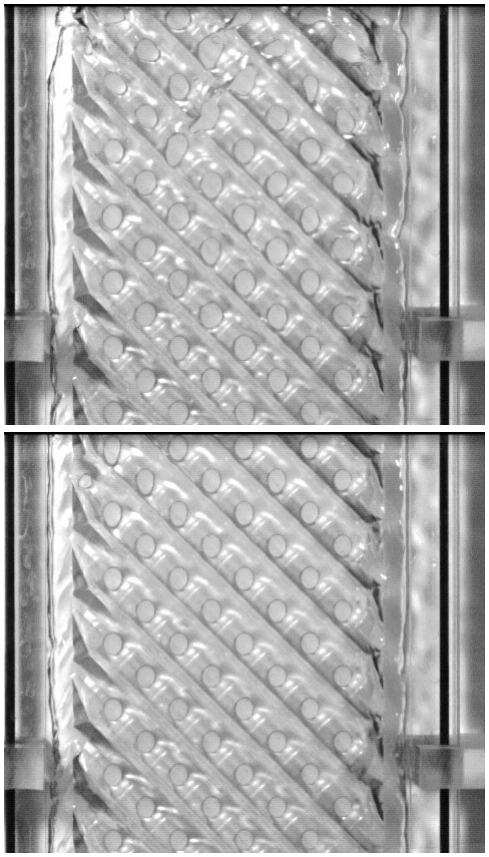

(a)

(b)

a) before flooding Q_L*= 0.028 l/s* Q_G *low*
b) "maldistribution" Q_L *= 0.028 l/s* Q_G *= 1.5 l/s*

Figure 2. Flow of water and air in corrugated-wall channel: a) counter-current flow and b) "maldistribution". Data corresponding to corrugated plates with side-grooves 9 mm wide.

In **Figure 2a**, it is evident that there are dry areas around the "contact points" (between peaks of the opposite corrugations), which seem to have an ellipsoidal shape changing randomly according to the flow development. As the gas flow rate increases the lateral drainage to the side channels (possibly aided by the gas shearing action) increases leading to a progressive elimination of the liquid film, covering the lower part of the corrugated channel. Indeed, it seems that the film is "wiped out" from that area. This is what one may define as liquid *"maldistribution"* in the channel. The observations suggest that the side grooves of the corrugated plates play a dominant role in liquid distribution; they tend to reduce the vertical downward motion of the liquid film by allowing the effective "drainage" of liquid that moves in the lateral direction, roughly along the valleys of the corrugations. It is evident (**Figures 2a and 2b**) that the dry regions around contact points tend to change their irregular ellipsoidal shape to a more uniform circular one as the gas flow rate increases. This change of shape is possibly related to the depletion/elimination of the liquid film (starting at the lower part of the plates and extending upwards), whereas drainage continues through the side grooves. By further increasing the gas flow rate, part of the liquid is swept up the channel, passing beyond the liquid injection region and generating a sustained concurrent up-flow. This condition is considered as the onset of *flooding*. Periodicity is evident in this churn type of upward motion of the liquid phase.

Flow patterns for air-kerosene counter-current flow is shown in **Figure 3**. In contrast to the water case, the dry areas at the "contact points", for kerosene as the liquid phase, seem to decrease in size possibly because of its lower surface tension and contact angle. These properties of kerosene tend to improve the wettability of Plexiglas and to cause a significant reduction of the flooding gas velocity.

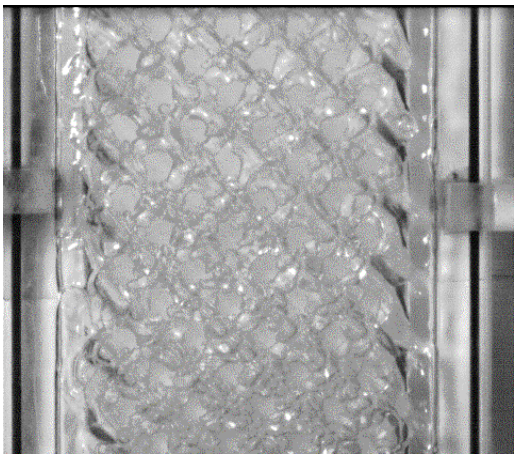

Figure 3. Kerosene with air (Q_L= 0.033 l/s, Q_G=0.5 l/s). Corrugated plates with side grooves 9 mm wide.

Another apparent feature of the runs with kerosene is the more chaotic flow pattern even at the upper part of the channel, in contrast to the water case where a uniform film/flow pattern was observed even at high gas velocities. Additionally, for the kerosene case, there is no noticeable critical condition for "maldistribution", whereas at the onset of flooding liquid seems to continue moving vertically downwards crossing corrugations; i.e. there is limited depletion of the film in the lower part of the channel.

Critical Flooding Velocities

The superficial gas velocity, U_G, used throughout the calculations for the corrugated wall case is defined as the volumetric flow rate of the gas phase divided by the cross sectional area of the flow channel. The latter is determined by precisely measuring the volume of water needed to fill a known height of the channel. an equivalent gap width, D_e, is calculated by using the measured cross sectional area and the corresponding wetted perimeter of the channel.

Figure 4 shows data for the air/water system. The superficial gas velocity U_G and volumetric flow rate, Q_G, at the onset of flooding, are plotted as a function of liquid mass flow rate per unit channel width, Γ_L, for three values of the *side* channel width (groove), i.e. 9, 4 and 0 mm. The last value corresponds to totally eliminating the grooves. The uncertainty in the measurements of the flooding velocity is estimated to be between 5 and 10%. The maximum corresponds to the lower flooding velocities. It is evident that the

flooding gas flow rate is strongly dependent on the size of the grooves, exhibiting a decrease as the width of the side channels decreases. This trend is due to the decrease of the liquid drainage in the lateral direction as a result of the reduction of the side channel area available for flow. Therefore, the air flow necessary for the onset of flooding (for a certain liquid flow rate) tends to decrease.

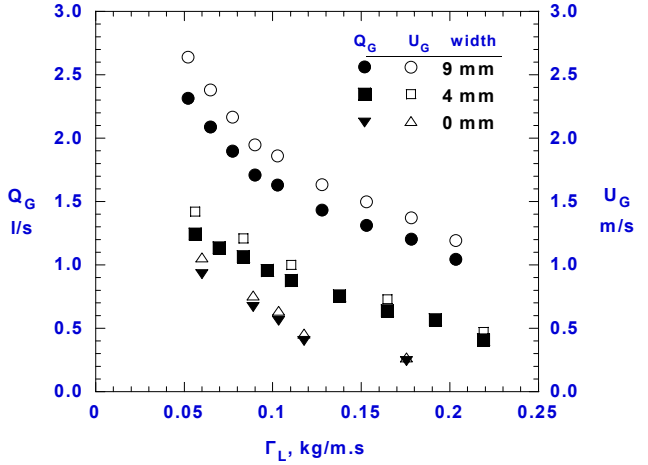

Figure 4. Gas velocity and flow rate plotted vs the liquid mass flow rate per unit channel circumference, Γ_L, at the onset of flooding, for various side channel widths.

Flooding data for three liquids i.e. water, butanol-water solution (5%) and kerosene are presented in **Figure 5**. Both the butanol solution and kerosene display flooding at lower air velocities than water because of their lower densities as well as their greater viscosities and lower surface tension and contact angle compared to those of water.

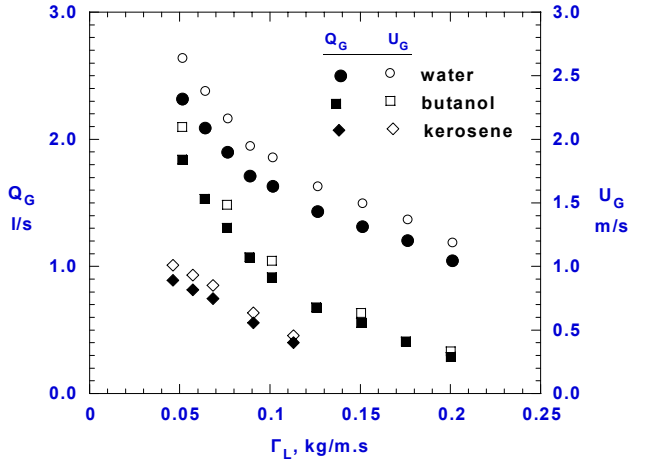

Figure 5. Gas velocity and flow rate plotted vs the liquid mass flow rate per unit channel circumference, Γ_L, at the onset of flooding, for various liquids. Data corresponding to corrugated plates with side-channels 9 mm wide.

Figure 6 shows a comparison of the experimental flooding data for smooth wall, with 5 and 10 mm gaps (Vlachos et al, 2001), and corrugated wall channels, for the air-water system. The corrugated-wall data correspond to vertical side-channels 9 mm wide. In order to compare and to correlate the set of data for the corrugated wall channel, a 5 mm equivalent gap has been selected. This value corresponds to the gap between the two plates at a point below the liquid entrance and right above the corrugations where the flooding appears to be initiated. The proximity of the corrugated surfaces (with distributed contact points), promoting extensive bridging of falling liquid layers, may be responsible for the much smaller critical flooding velocities observed, compared with the flat-wall channels.

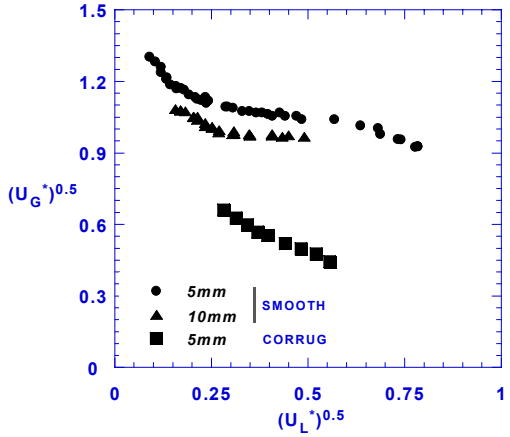

Figure 6. Comparison of experimental flooding data for air/water and two types of channels; i.e. smooth plates (gap 5mm and 10mm) and corrugated-wall plates with side grooves 9mm wide (equivalent gap 5mm)

An attempt to correlate the flooding data for corrugated-wall channels, for the three liquids tested, in terms of the dimensionless gas Reynolds, Froude and Ohnesorge numbers (defined below) is presented in **Figure 7**. It is interesting that the gas Reynolds number, Re_G, at incipient flooding, is a nearly linear function of the product $Fr_L^{0.15}Oh_L^{0.3}$. It is also worth mentioning that the liquid with the highest Ohnesorge number exhibits flooding at lower gas velocities. The Reynolds, Re_G, Froude, Fr_L, Ohnesorge, Oh_L, and Kapitza, Ka_L, dimensionless numbers are defined below:

$$Re = \frac{D\ U_G}{\nu}, \qquad Fr_L = \frac{\rho_L U_L^2}{gD\Delta\rho},$$

$$Oh_L = \sqrt{\frac{\mu^2}{\rho D\sigma}}, \qquad Ka_L = \frac{\sigma}{(\nu g)^{1/3}\mu} \qquad (3)$$

The correlation in **Figure 7** may be represented by

$$Re_G = 2.3\times10^3 - 1.86\times10^4\ [Fr_L\ Oh_L^2]^{0.15} \qquad (4)$$

Figure 7 provides also an indication that the expression

$$[Fr_L\ Oh_L^2]^{0.15} < 0.13 \qquad (5)$$

may be a general criterion (more specifically an upper-limit) to avoid flooding in corrugated plate condensers of the type tested here. More tests with other geometries and fluids are required to assess the reliability of expressions (4) and (5).

Pressure Drop in Channel with Corrugated Walls

Values of mean (time averaged) pressure gradient, measured between the lower and the upper limit of the corrugated channel are presented in **Figure 8** for various air and water flow rates. As expected, the pressure drop tends to increases with the air flow rate. An increase in pressure drop with liquid flow rate is observed as well. The occurrence of flooding is associated with a rather sharp increase in pressure gradient. Moreover, there is also a narrow range of gas flow rates where the pressure drop tends to be nearly independent of the gas flow rate. This range corresponds to the situation previously referred to as "maldistribution", where (as seen in the video recordings) the air flows over (at least part of) the corrugated walls of the channel inade-

quately wetted by water; i.e. the water has drained to side-grooves.

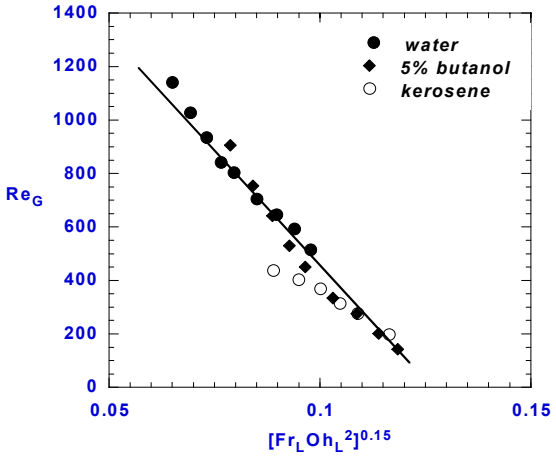

Figure 7. Flooding conditions for various liquids expressed by dimensionless groups. Data corresponding to corrugated channels with side-grooves 9 mm wide.

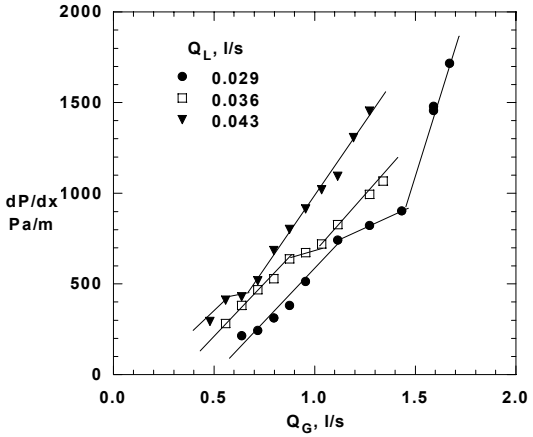

Figure 8. Mean pressure drop values for counter-current flow air/water flow. Corrugated-wall channel with side grooves 9 mm wide.

The time series of the pressure drop were statistically analyzed to obtain the RMS values and hence the intensity of the pressure drop fluctuations, which is defined as the percent ratio of the RMS values over the corresponding mean value of the pressure drop. In **Figure 9** the *intensity* of the pressure fluctuations is plotted versus the gas flow rate for various liquid rates. It is apparent that at the lower gas velocities the intensity attains its maximum values, whereas for high gas velocities it tends to approach a constant value. Moreover, the intensity of the fluctuations tends to decrease by increasing the liquid flow rate.

The calculated *power spectra* of the pressure drop fluctuations for air-water experiments are presented in **Figure 10**, for a typical liquid flow rate and for two conditions i.e. "maldistribution" and flooding. A very pronounced maximum, at frequencies between 5 and 8 Hz is observed for the "maldistribution" and flooding conditions. There is also evidence from the video recordings that this dominant frequency corresponds to the periodic upward motion of the liquid near the liquid entrance, at the onset and during the liquid flow reversal. The second distinct but less pronounced peak at about 30 Hz is apparently related to a characteristic frequency in the operation of the vacuum pump and it is present in all experiments. Some tests done in the absence of vacuum pumping action tend to confirm this interpretation.

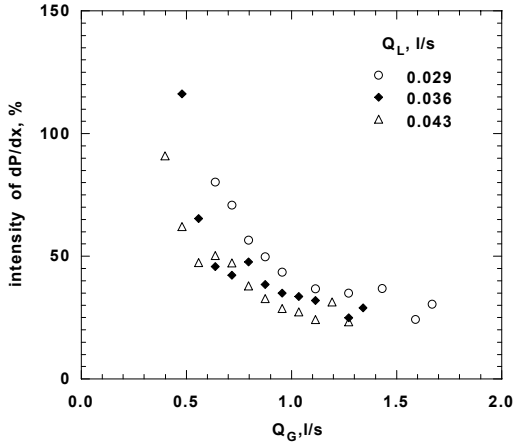

Figure 9. Intensities of pressure drop fluctuations for counter-current flow including flooding

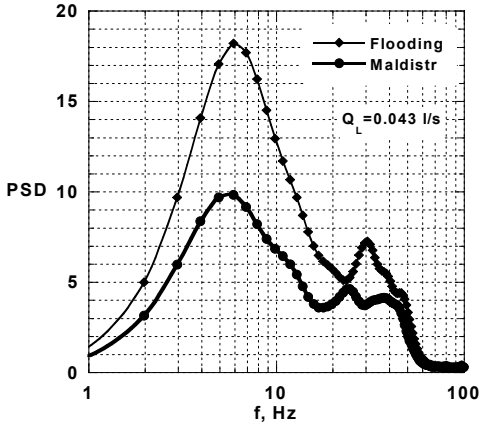

Figure 10. Pressure drop fluctuation spectra for counter-current flow (CCF) and during flooding.

Mean (time averaged) pressure gradient data for air-water, air-5% butanol solution in water, air-kerosene are presented in **Figure 11**. It is pointed out that the data shown in this graph correspond to the counter-current flow condition, near the "maldistribution" critical point (away from the flooding conditions). The meager data collected for kerosene are due to the low flooding gas velocities and the small flow rates away from the onset of flooding attainable in the experimental set-up. The same general trend as for air-water flow is observed for both the butanol solution and kerosene. An increase in pressure drop with liquid volumetric flow rate is observed as well. However, compared to water, a steeper increase of the pressure gradient is evident for butanol and kerosene.

The measured pressure drop may be expressed (Eq.6) in terms of a friction factor f_G, and an attempt was made for data correlation by an expression containing the dimensionless groups Re_G (gas Reynolds number) and Ka_L (Kapitza number), the latter to take into account the fluid physical properties.

$$\frac{dP}{dx} = \frac{2 f_G \rho_G U_G^2}{D} \qquad (6)$$

The experimental friction factor values, plotted against the dimensionless group $Re_G(Ka_L)^{0.5}$, show some correlation only at large values of this group ($>10^4$). In the absence of other literature models or expressions, a Lockhart-Martinelli

type correlation, applied to co-current flow in corrugated channels (Winkelman et al, 1999), was also used to check the new data. That correlation predicts much higher pressure drop compared to measurements.

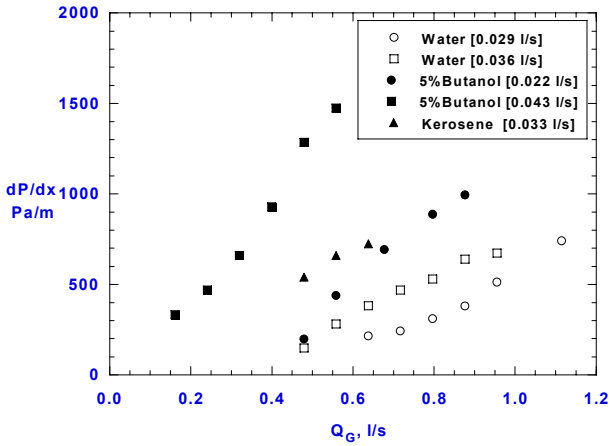

Figure 11. Pressure drop vs. gas flow rate for various liquids. Values in brackets represent liquid flow rate.

4. CONCLUDING REMARKS

The observations suggest that the vertical side grooves play a dominant role in flow distribution, allowing the effective "drainage" of liquid moving in the lateral direction, roughly along the valleys of the corrugations. Two critical flow conditions were identified, which are of considerable practical significance:

At a certain gas flow rate, lateral "drainage " to the side channels is apparently aided by the gas shearing action, thus almost totally depleting of liquid the lower part of the plates. This type of liquid distribution which is referred to as "maldistribution" may be favourable for the operation of such a device as a condenser because of the exposure of nearly 'fresh' wall to the condensing vapors. At higher gas velocity, this liquid depletion extends upwards and partial liquid flow *reversal* is observed in the upper part of the plates while drainage continues through the side channels. This is considered as the condition of incipient flooding. It is interesting that much higher flooding velocities are observed with flat-wall channels, compared to corrugated-wall passages under equivalent conditions.

The critical gas velocities of incipient "maldistribution" and of flooding tend to increase with decreasing liquid rate, as expected. Concerning fluid properties, significant differences are observed (compared to water) in the liquid film distribution and the flooding velocities with the lower interfacial tension butanol solution and kerosene. The latter are associated with the smallest measured flooding velocities.

The pressure drop tends to increase with both the air and the liquid flow rates. The occurrence of flooding is associated with a rather sharp increase in pressure gradient. Moreover, there is also a narrow range of gas flow rates where the pressure drop is nearly independent of the gas flow rate and which corresponds to the "maldistribution". Compared to water, a sharper increase of the pressure gradient is evident for the butanol mixture in the same range of flow conditions. The intensity of the pressure fluctuations attains its maximum values at the lower gas velocities, whereas it tends to move toward a constant value for higher velocities. Furthermore, this intensity tends to decrease with increasing liquid flow rate.

Acknowledgment Financial support by the European Commission under contract JOE3-CT97-0062 is gratefully acknowledged

5. REFERENCES

Bankoff, S.G. and Lee, S.C. 1986 A critical review of the flooding literature. In *Multiphase Science and Technology*, Chapter 2 (*Edited by* Hewitt, G.F., Delhaye, J.M. and Zuber, N.), pp. 95-180. Hemisphere, New York.

Biage, M. 1989 Structure de la surface libre d'un film liquide ruisselant sur une plaque plane vertical et soumis a un contre-courant de gas: Transition vers l'ecoulement cocourant ascendant. Ph.D. Thesis, Inst. Nat. Polytechnique de Grenoble, France.

Ghiaasiaan, S.M., Wu, X., Sadowski, D.L. and Abdel-Khalik, S.I. 1997 Hydrodynamic characteristics of counter-current two-phase flow in vertical and inclined channels: effects of liquid properties. *Int. J. Multiphase Flow* **23**, 6, 1063-1083.

Koizumi, Y. and Ueda, T. 1996 Initiation conditions of liquid ascent of the counter-current two-phase flow in vertical pipes (in the presence of two-phase mixture in the lower portion). *Int. J. Multiphase Flow* **22**, 1, 31-43.

Larson, T.K., Oh, C.H. and Chapman, J.C. 1994 Flooding in a thin rectangular slit geometry representative of ATR fuel assembly side-plate flow channels. *Nucl. Eng. Des.* **152**, 277-285.

Lacy, C.E. and Dukler, A.E. 1994 Flooding in vertical tubes – Part I: Experimental studies of the entry region. *Int. J. Multiphase Flow* **20**, 2, 219-233.

Osakabe, M. and Kawasaki, Y. 1989 Top flooding in thin rectangular and annular passages. *Int. J. Multiphase Flow* **15**, 5, 747-754.

Vlachos, N.A., Paras, S.V., Mouza, A.A. and Karabelas, A.J. 2001 Visual observations of flooding in narrow rectangular channels. *Int. J. Multiphase Flow* **27**, 8, 1415-1430.

Wallis, G.B. 1969 One-dimensional two-phase flow, McGraw-Hill, New York.

Winkelmann, D., Thonon, B., Auracher, H. and Bontemps, A. 1999 Two-phase flow characteristics of a corrugated channel. *20th International Congress of refrigeration, IIR/IIF, Sydney* .

Wongwises, S. and Thanaporn, P. 1998 Heat-mass transfer and flow characteristics of two-phase counter-current annular flow in a vertical pipe. *Int. Comm. Heat Mass Transfer, **25**, 819-829.*

Yan Y.Y., Lio, H.C. and Lin, T.F. (1999) Condensation heat transfer and pressure drop of refrigerant R-134a in a plate heat exchanger. *Int. J. Heat & Mass Transfer, **42**, 993-1006.*

Zapke, A. and Kroeger, D.G. 2000a Counter-current gas-liquid flow in inclined and vertical ducts – I: Flow patterns, pressure drop characteristics and flooding. *Int. J. Mult. Flow, **26**, 1439-1455.*

Zapke, A. and Kroeger, D.G 2000b Counter-current gas-liquid flow in inclined and vertical ducts – I: The validity of the Froude-Ohnesorge number correlation for flooding. *Int. J. Mult. Flow , **26** , 1457-1468.*